

# Referent 3D solid tumour model and absorbed dose calculations at cellular level in radionuclide therapy

Spaic R<sup>1</sup>, Ilic R<sup>2</sup>, Petrovic B<sup>3</sup>, Dragovic M<sup>3</sup>, Toskovic F<sup>3</sup>

<sup>1</sup> Institute of Nuclear Medicine, Medical Military Academy, Crnotravska 17, 11000 Belgrade, Serbia and Montenegro

<sup>2</sup> Institute of Nuclear Science VINCA, 11001 Belgrade, Serbia and Montenegro

<sup>3</sup> Faculty of Organisation Sciences, Jove Ilica 161, 11000 Belgrade, Serbia and Montenegro

## Abstract

An average absorbed dose of the tumour calculated by the MIRD formalism has not always a good correlation with the clinical response. The basic assumption of the MIRD schema is that a uniform spatial dose distribution is opposite to heterogeneity of intratumoral distribution of the administered radionuclide which can lead to a spatial non-uniformity of the absorbed dose. Therefore, in clinical practice, an absorbed dose of the tumour at the cellular level has to be calculated. The aim of this study is to define a referent 3D solid tumour model and using the direct Monte Carlo radiation transport method to calculate: a) absorbed fraction, b) spatial 3D absorbed dose distribution, c) absorbed dose and relative absorbed dose of cells or clusters of cells, and d) differential and accumulated dose volume histograms. A referent 3D solid tumour model is defined as a sphere which is randomly filled with cells and necrosis with defined radii and volumetric density. Radio-labelling of the tumour is defined by intracellular to extracellular radionuclide concentration and radio-labelled cell density. All these parameters are input data for software which generates a referent 3D solid tumour model. The modified FOTELP Monte Carlo code was used on this model for simulation study with beta emitters which were applied on the tumour. The absorbed fractions of Cu-67, I-131, Re-188 and Y-90 were calculated for different tumour sphere masses and radii. Absorbed doses of cells and spatial distributions of the absorbed doses in the referent 3D solid tumour were calculated for radionuclides I-131 and Y-90. Dose scintigram or voxel presentation of absorbed dose distributions showed higher homogeneity

for Y-90 than for I-131. A differential dose volume histogram, or spectrum, of the relative absorbed dose of cells, was much closer to the average absorbed dose of the tumour for Y-90 than I-131. An accumulated dose volume histogram showed that most tumour cells received a lower dose than average, or prescribed, tumour absorbed dose. Those discrepancies between conventional and cellular approach show that dosimetry on the cellular level is necessary for a better selection of the radionuclide and optimal calculation of administered activity in the radionuclide therapy.

**Key words:** dosimetry, radionuclide therapy, Monte Carlo simulations, absorbed fraction, dose volume histogram

**World J Nucl Med 2007;6:45-51**

## Introduction

The main goal of dosimetry in the radionuclide therapy is calculation of the prescribed tumour absorbed dose and critical organ accuracy (1,2). This is related to radionuclide selection and optimization of the administered activity and estimation of the clinical response and potential benefit for the patient (3-5). The MIRD schema as the most common method applied in the radionuclide therapy calculates the average absorbed dose of tumour and critical organs (6). This conventional approach uses macroscopic characteristics of tumour and introduces some acceptations (7). The average tumour absorbed dose mostly does not correspond to clinical response. The main reason for that is the basic assumption of the MIRD schema that the spatial distribution of the administered activity and calculated absorbed dose were uniform.

Heterogeneity of intratumoral distribution of administered radionuclides leads to non-uniformity of the absorbed dose (8-11). It means that in clinical practice calculations of an absorbed dose of the tumour at the cellular level are necessary (12-14). Three methods can be used for tumour dosimetry calculations: a) dose point-kernel convolution, b) S-values, and, c) direct Monte Carlo radiation transport. Only direct Monte Carlo radiation transport method can be used for tissue with different composition and density (15). Self and cross doses have been defined and calculated, but

## Correspondence:

Mr. Rajko Spaic

Medical physicist

Medical Military Academy

Institute of Nuclear Medicine

Crnotravska 17, 11000 Belgrade

Serbia and Montenegro

E-mail: voxel@eunet.yu

this approach has not offered clinicians satisfactory tools for the radionuclide therapy planning (16).

Tumour absorbed dose calculations require a method which includes all tumour characteristics. For that reason a wide spread of all physical, physiological, radiopharmacological, histological and other clinical parameters relevant for the tumour and the patient must be used. The cellular dosimetry system had to calculate the absorbed dose of cells or cluster of cells and spatial 3D distribution of the absorbed dose in the tumour volume. For the purpose of comparing conventional and cellular dosimetry we defined a relative absorbed dose of cells.

A reference man has been defined in the conventional dosimetry (17). We found that in the cellular dosimetry the referent tumour and normal organ with cellular morphometry and all other relevant parameters had to be defined. The referent 3D solid tumour model at the cellular level was introduced to improve the radionuclide therapy and also to standardise the absorbed dose calculations. The referent 3D solid tumour model could be arranged to be patient specific if histopathological data were used for the specific tumour morphometry and imaging technique for calculating the tumour size and volume for the given patient.

The planning systems in the radionuclide therapy have mainly been using the conventional approach (18). Our goal is to include this model and the absorbed dose calculation at the cellular level as a part of the planning systems in the radionuclide therapy. It will be an inverse planning system, which means that for the prescribed tumour absorbed dose this system must select an appropriate radionuclide and calculate the activity to be administered for specific radiopharmaceuticals and patients. Both spatial distribution of an absorbed dose at the cellular level and differential and accumulated dose volume histograms (DVHs) will contribute to a better radionuclide selection and administered activity optimization leading to the best radionuclide therapy plan.

## Materials and methods

### Referent tumour morphometry

Tumour morphometry is complex. Referent morphometry values which are part of the referent 3D solid tumour model must include all relevant parameters of the tumour type and growth. This morphometry must be generated as realistic as possible presentation of the tumour and provide a virtual generation of all specific tumours. The crucial moment of interest in a tumour growth pattern, for the radionuclide therapy, is the moment of its diagnostic detectability. Nowadays diagnostic imaging techniques allow faster tumour detection, enabling clinicians to start a therapy earlier. At that moment we define the referent 3D solid tumour model as a sphere with a radius  $R$  ( $\mu\text{m}$ ) filled with cells or a cluster of cells as spheres, and with an extracellular space. Virtual cells with medium radius  $r$  ( $\mu\text{m}$ )

and standard deviation  $d$  ( $\mu\text{m}$ ) are randomly placed in the tumour space one by one. Cellular volume density  $c$  (%) of the tumour is defined as the total cells volume divided by the tumour volume. The referent 3D solid tumour model defined in that moment we call Level Zero. In a certain later moment of the tumour growth we can define Level A of the referent 3D solid tumour with one spherical necrosis located in the centre of the tumour with a defined radius. Level B of the referent 3D solid tumour includes a lot of spherical necroses with the medium radii, standard deviation and linear decrease distribution from the centre to the periphery of the tumour. The volume of necrosis in the referent 3D solid tumour model is defined with necroses density  $n$  (%). Necroses density for Level Zero is zero. A referent solid tumour with virtual cells is presented in 3D mode, using RasTop code (19). The tissue composition and density of virtual cells and extracellular space can be selected from the materials database or custom defined. For all simulations in this study, done with Level Zero referent 3D solid tumour model, we used a soft tissue chemical structure (20).

### Radionuclide labelling

The radionuclide, applied in a virtual tumour, can remain in cells or in the extracellular space. The parameter called intracellular to extracellular radionuclide concentration  $k$  (%), defined this activity ratio. Radionuclide was deposited in certain percentage of tumour cells defined by the parameter called labelled cell density  $f$  (%). Those two parameters determined nonhomogeneity of the radionuclide distribution in the tumour (7). We used homogeneous radioactivity labelling within entire cell volume. On the subcellular level the labelling of radioactivity could be homogeneous in: a) nucleus, b) cytoplasm, c) membrane. Simulations presented in this paper were done with homogeneous distribution of activity in the cell volume.

### Monte Carlo simulation

Many approaches and computer programs are used in absorbed dose calculations (21-23). Monte Carlo simulations are mostly applied by various software codes and calculation methods (24,25). Voxel Monte Carlo simulations are state of art in this moment (26,27). The software package FOTELP has been developed to simulate the transport of photons, electrons and positrons by the Monte Carlo method for numerical experiments in dosimetry, radiotherapy and other applications (28). Codes from this package perform calculations in 3D geometry with random spectra of particles, having energy in the range from 1 keV to 100 MeV, and material zones which could be described by planes and surfaces of the second order (29). FOTELP codes used transition probabilities from the previous to the following state of phase space previously prepared by FEPDAT code (28).

Photon transport was based on the imitation model (30,31). During the photon history, from one to the another collision, random values of the following parameters were chosen from the corresponding distribution: distance, target (atom,

shell), collision type, type of secondary particles, energies and angles of particles after collision. FOTELP code treated photoelectric absorption, incoherent scattering, electron-positron pairs generation and coherent scattering. Secondary photons from the bremsstrahlung radiation, fluorescent photons and photons from positron annihilations were included as photons from the source.

Electron and positron transport was based on the theory of condensed history on the part of the particle range (28,30). Mean energy loss was determined in that range with its fluctuation by Landau (32), i.e. Blunck-Leizegang distribution (33). Under the conditions of the multiple scattering theory, the particle deviation angle was chosen from Moliere (34) or Goudsmit-Saunderson (35) distributions. Bremsstrahlung was generated from Poisson distribution and spectrum of photon emission. Production of delta electrons on the range was generated from Poisson distribution, while energy distribution was based on Moller and Bhabha cross section (36). The angles of the secondary particles in electron-positron transport were chosen from relevant distributions. Photoelectric absorption and impact ionisation were followed by a simulation of atomic transitions on six levels and generated fluorescent photons. Auger electrons were treated as relevant particles from the source.

For the purposes of this investigation FOTELP code was improved with: a) tumour morphometry generation in combined geometrical RFG module with Rvachev functions; b) implementation of radioactive sources in the tumour volume: homogeneously in labelled cells and extracellular space, or at subcellular level homogeneously in the nucleus, cytoplasm or membrane. FOTELP code written in Fortran 77 and carried out on a standard PC could perform simulations with referent 3D solid tumour model containing up to eight hundred cells. Simulation run time depended on referent tumour parameters, applied radionuclide and activity ranging from a few minutes to several hours.

#### **Radionuclides**

This model was made for the radionuclide therapy and, because of that, all simulations were done with radionuclide, not with a monoenergetic particle. Radionuclides had a different number of beta emissions, electrons and photons. For electrons and photons each initial particle started with the same energy. For beta emitters, each initial particle started with medium energy. Energies (MeV) for electrons and photons, medium energy (MeV) for beta emissions and probabilities of those events were obtained from tables (37). In that way the radionuclide activity (Bq) was transformed into a sum of events of the particles (photons or electrons).

#### **Cellular dosimetry model**

The absorbed fraction in the MIRD schema is defined as the fraction of the energy emitted by the source organ that is absorbed in the target organ. Dosimetry in the radionuclide therapy began with the absorbed fraction i.e. with

calculation energy, emitted per decay and deposited in the tumour (38,39). The referent 3D solid tumour model and Monte Carlo simulations allow such calculations. When the fraction of the energy that remains in the tumour was known, then it is necessary to calculate: a) absorbed doses per cells, and b) spatial distribution of the absorbed dose at cellular level. The absorbed dose per cell was defined as total energy from all sources in the tumour absorbed in cell, divided by its mass. The absorbed dose was calculated for all tumour cells and presented as a histogram. Spatial distribution of the absorbed dose was defined as the energy deposited in the element of the tumour volume divided by its mass and presented as images with a standard voxel space resolution being  $R(\text{im})/100$ . The absorbed dose images of slices of the referent tumour we called dose scintigrams.

The average tumour absorbed dose was also calculated using Monte Carlo FOTELP code, but on the conventional level, meaning that the activity was homogeneously distributed within the tumour volume. The relative absorbed dose of a cell was defined as the absorbed dose of that cell, divided by an average tumour absorbed dose. Differential and accumulated DVHs were generated from the simulation data on the referent 3D solid tumour model. Differential DVH was generated as a spectrum of the relative absorbed doses of the cells. Accumulated DVH represented all tumour cells with certain relative absorbed dose.

#### **Radionuclide therapy planning system at cellular level**

The referent 3D solid tumour model can be a part of the radionuclide therapy planning system for specific patients (40,41). The first part of this system is the test scintigraphy module which calculates accumulated activity in the tumour (42). The second, a geometry module, which consists of the test computer tomography or magnet resonance images to calculate the tumour volume. The third, a morphometry module calculates specific tumour morphology, using histopathology data. All test images were transferred from equipment to radionuclide therapy work station by DICOM standard. The next step is the calculation of absorbed doses of the cells and their spatial distribution in the generated tumour with a specific volume and morphometry. Final results can be presented using differential and accumulated DVHs.

#### **Results**

A graphic presentation of cells in the referent 3D tumour model and their absorbed doses for radionuclides I-131 and Y-90 is given in Figure 1. Radiolabeled cells are coloured red and non-labeled cells blue. By zooming and rotation of RasTop code images it is possible to see how the tumour volume is filled with cells and to verify that there is no overlapping. The tumour growth is characterized by necrosis density (Level A and B). The number of cells in the referent 3D tumour model on Level Zero (without necrosis)

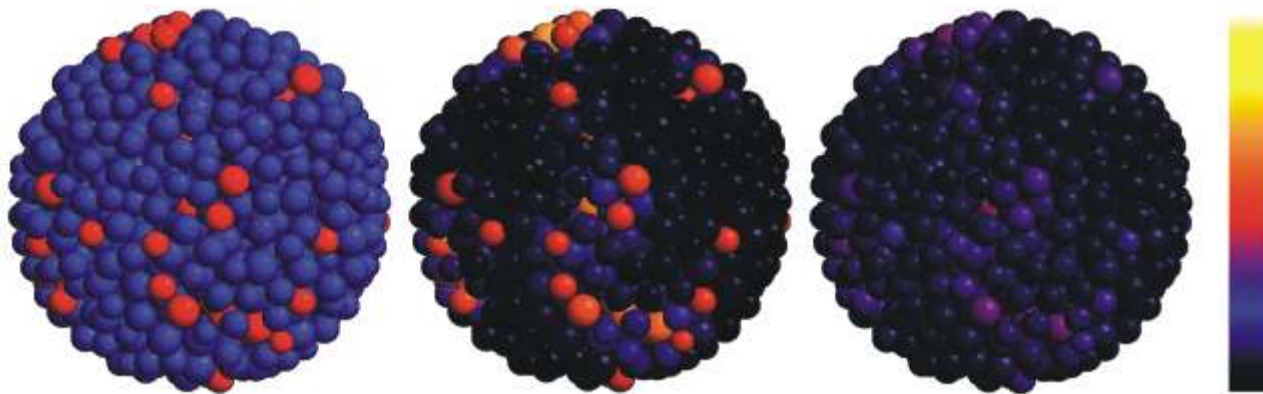


**Figure 1.** Graphical presentation of referent 3D solid tumour model in RasTop code (left), and absorbed doses in cells for radionuclides I-131 (middle) and Y-90 (right) in colour combinations. Radius of tumour 1000  $\mu\text{m}$ , median radii of cells 80  $\mu\text{m}$  (SD=8  $\mu\text{m}$ ). Volumetric cell density = 40%, Percentage of labelled cells = 10%. Total number of cells = 802. Applied activity = 3.7 MBq. Ratio of intracellular to extracellular activity = 0.9. Activity is homogeneously distributed in labelled cells and in extracellular space.

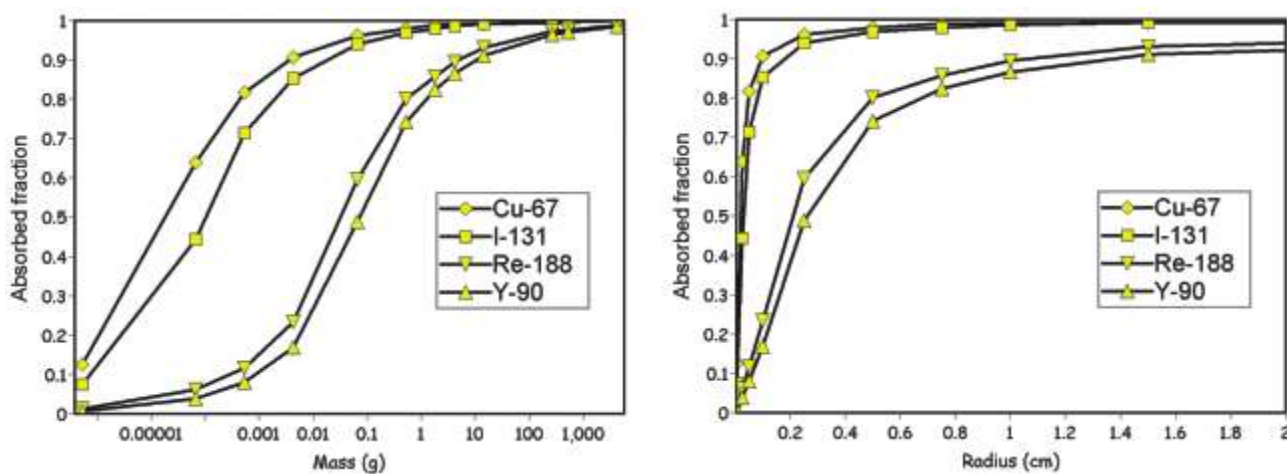


**Figure 2.** Absorbed fraction in tumour spheres is a function of mass (left) and radius (right) for beta emitting radionuclide. Absorbed fraction is calculated only for beta particles and electrons (Photons are excluded from calculations). Activity of radionuclide is homogeneously distributed in tumour spheres with soft tissue density.

Volumetric cell density (%)	Median radius and standard deviation of cells ( $\mu\text{m}$ )				
	25 $\pm$ 10	50 $\pm$ 20	100 $\pm$ 40	200 $\pm$ 80	400 $\pm$ 160
10	4,450.903	556,079	69,398	8,671	1,053
20	8,906.649	1,112.399	138,455	17,300	2,190
30	13,353.205	1,669.777	207,907	25,927	3,313
40	17,804.216	2,227.011	278,734	34,673	4,366
45	20,029.094	2,504.724	313,216	39,188	4,896

**Table 1.** Number of cells in referent 3D solid tumour model for different cell densities and radii. Radius of tumour sphere 10,000  $\mu\text{m}$

is given in Table-1. The radii of the cells have normal distribution. The referent tumour is completely defined when all parameters are set. Volumetric cell density higher than 45% is very hard to achieve. For cell densities lower than 40%, the time of computer generation of the referent 3D solid tumour is a few seconds.

The absorbed fractions in function of the tumour mass, and radii for radionuclides Cu-67, I-131, Re-188 and Y-90 are given in Figure 2. The absorbed fractions are calculated for

monoenergetic electrons and beta emitters (photon energy not included) and with homogeneous, uniform radionuclide distribution in the referent tumour sphere, mass ranging from 0.000001 to 1000 g, and tumour sphere radii ranging from 10  $\mu\text{m}$  to 2 cm. As for small tumours, most energy leaves the tumour, but as the tumour radius grows, the percentage of energy deposited in the tumour volume also grows. Tracers, with low beta energies such as Cu-67 and I-131, deposit a larger percentage of energy in the tumour

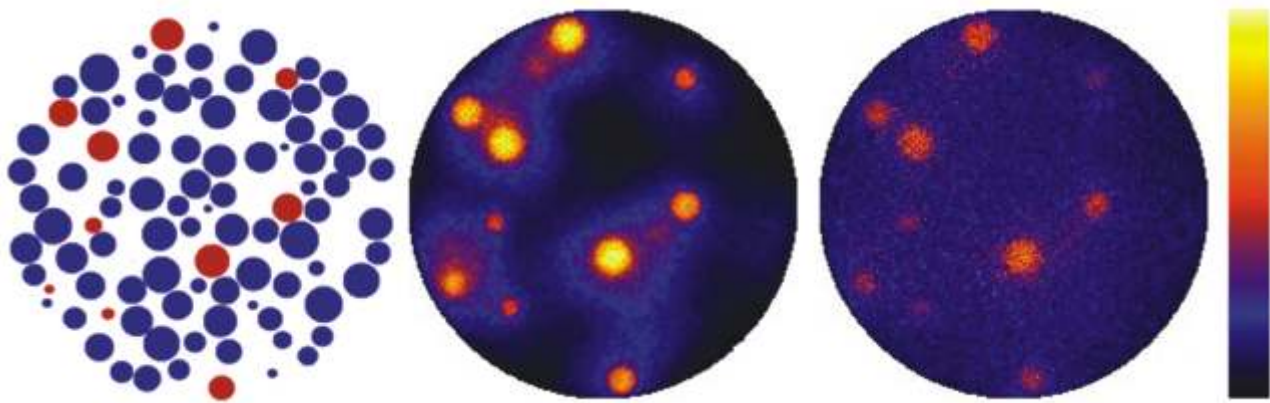


**Figure 3.** One slice of the same referent 3D solid tumour model (left) and spatial distribution of absorbed doses in that slice for I-131 (middle) and Y-90 (right), with color scale. Voxel space resolution is 10  $\mu\text{m}$ .

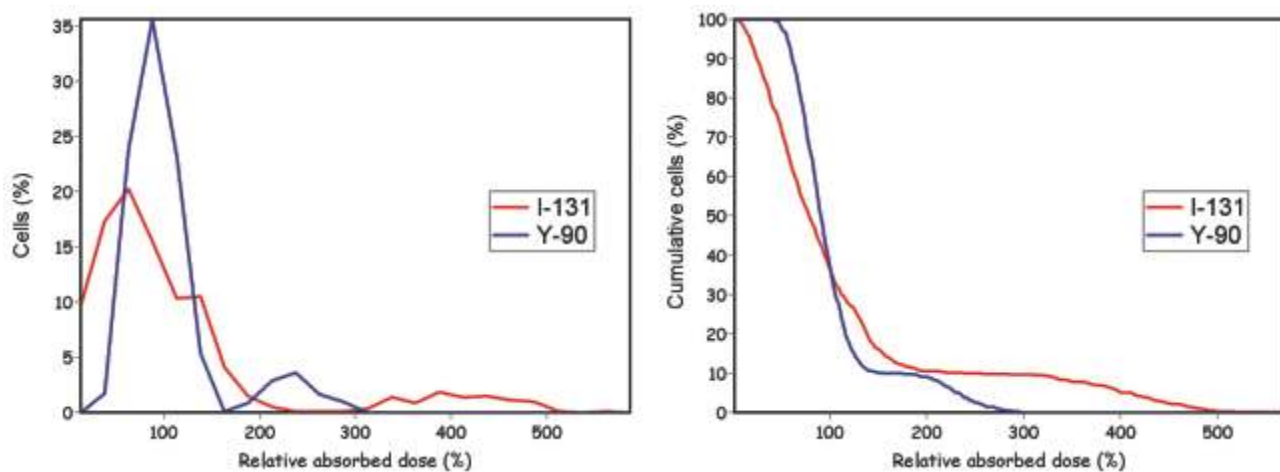


**Figure 4.** Differential (left) and accumulated (right) DVHs for I-131 and Y-90. Both DVHs were generated from same simulation on referent 3D solid tumour model.

volume than those with high energy beta emitters, such as Re-188 and Y-90. With more massive solid tumours this difference decreases.

A dose scintigram or absorbed dose spatial distribution of the referent 3D solid tumour for radionuclides I-131 and Y-90 is given in Figure 3. The absorbed doses calculated for all voxels and slices of the tumour cross section were generated. Simulations were done on the referent tumour for the applied radionuclide, and with the same morphometry and labelling parameters. As spatial distribution of the absorbed dose in the referent tumour was non-uniform, the labelled cells received much higher doses than non-labelled. Dose scintigram with applied Y-90 showed much more homogeneity.

The relative absorbed dose per cell for the referent tumour, with administered radionuclides I-131 and Y-90, was calculated for the unit activity deposited in the tumour and is represented as differential and accumulated DVHs respectively in Figure 4. Differential DVH shows that there is one peak for the labelled and another for non-labelled cells. Both peaks for high energy beta emitters are closer to average tumour absorbed dose. A great number of cells have relative absorbed dose values smaller than one

hundred, meaning that they receive less absorbed doses than average. Accumulated DVH for applied I-131 on Level Zero referent 3D solid tumour model is very far from ideal. DVH for applied Y-90 is much better than that of I-131.

## Discussion

The referent 3D solid tumour model has been established for the purpose of calculation of the absorbed dose at the cellular level and for standardisation of different calculation methods. Our model includes estimated levels of tumour progression that correspond to the growth pattern and simulate a different tumour type using defined morphometry parameters. Radionuclide labelling on the cellular and sub-cellular level is included in the model (43). This is reference based system, but, using patient's histopathological data for tumour morphometry and imaging technique for calculating the tumour size, volume and accumulated activity, it becomes a patient specific dosimetry system.

Using this model, and Monte Carlo simulations, with FOTELP code, absorbed fractions of electron and beta

particles energy for sources uniformly distributed in spheres of various sizes, were calculated (Figure 2). For small spheres, small tumours and micrometastases, the electron energy which escapes the tumour volume cannot be neglected and must be calculated for the specific radionuclide, tumour mass and shape (Figure 2a). The upper limit for an absorbed fraction, as defined in the MIRDSchema, is the asymptote value that can be achieved only for spherical tumours with very big radii (Figure 2b). The absorbed fractions in tumours with small radii are greater with low energy beta emitters. Absorbed fraction calculations could be compared with simulation results from other investigators and performed by different methods (44). The estimation of an absorbed fraction helps us in analysis but cannot be sufficient for the radionuclide selection.

Spatial distribution of the absorbed dose, or dose scintigraphy, is calculated for all slices of the spherical tumour volume (Figure 3). For high non-uniformity of accumulated activity in tumour, the absorbed doses must be calculated at the cellular level. The number of cells which received average absorbed doses using radionuclide with low energy beta emitters, such as I-131, is very small (45). That is one of the important reasons why conventional dosimetry and clinical response of radionuclide therapy are not in accordance. For high energy radionuclides, like Y-90, absorbed dose distribution is much more homogeneous and the influence of non-uniform activity distribution is smaller. This dose scintigraphy is very important for presentation of spatial distribution of the absorbed dose and its non-uniformity for specific radionuclide therapy.

Monte Carlo simulations with FOTELP code done on the referent 3D solid tumour model gave us differential and accumulated DVHs (Figure 4) as the best methods for the presentation of the cell dosimetry in the radionuclide therapy. Both DVHs showed that the tumour cell did not receive sufficient absorbed dose and something had to be done to improve this. With DVHs it was possible to present objectively the influence of different radionuclide, tumour morphometry and radiolabelling characteristics on the absorbed doses of cells. There was also a good and exact ratio between the prescribed absorbed dose and specific absorbed dose distribution on the cellular level in a tumour. When introduced in the clinical practice DVHs will put the radionuclide therapy plan on the same methodological level as the external radiotherapy.

Our model allows simulations with different geometric, morphometric, histopathological and radiolabelling parameters. Certain limitation of the referent model is that all shapes are spheres but specific shapes defined from histological data can be included in the model. The model can be further improved with a better implantation of the tumour growth, adding new parameters and a realistic dynamic model.

The referent 3D solid tumour model would be of help in optimisation of radionuclide selection for a specific tracer

and to the medical physicist who calculates the administered activity accuracy for the prescribed absorbed doses (46). The basic concept of treatment planning systems in the radionuclide therapy must be a generation of optimal DVHs for an individual therapy plan. With an absorbed dose calculation at the cellular level it is possible to achieve this goal and to improve clinical application of the radionuclide therapy.

## References

1. Stabin MG, Tagesson M, Thomas SR, Ljungberg M, Strand SE. Radiation dosimetry in nuclear medicine. *Appl Radiat Isot* 1999; 50:73-87
2. Zanzonico PB. Internal radionuclide radiation dosimetry: a review of basic concepts and recent developments. *J Nucl Med* 2000; 41:297-308
3. Humm JL. Problems and Advances in the Dosimetry of Radionuclide Targeted Therapy. *Recent Results in Cancer Research* 1996; 141:37-65
4. DeNardo GL, Juweid ME, White CA, Wiseman GA, DeNardo SJ. Role of radiation dosimetry in radioimmunotherapy planning and treatment dosing. *Critical Reviews in Oncology/Hematology* 2001; 39:203-218
5. Hartmann-Siantar CL, Vetter K, DeNardo GL, DeNardo S. Treatment planning for molecular targeted radionuclide therapy. *Cancer Biotherapy and Radiopharmaceuticals* 2002; 17:267-280
6. Loevinger R, Budinger T, Watson EE. *MIRD Primer for Absorbed Dose Calculations*, Revised. New York, Society of Nuclear Medicine 1991
7. Makrigiorgos GM, Adelstein SJ, Kassis AI. Limitations of conventional internal dosimetry at the cellular level. *J Nucl Med* 1989; 30:1856-1864
8. Howell RW, Rao DV, Sastry KS. Macroscopic dosimetry for radioimmunotherapy: non-uniform activity distributions in solid tumours. *Med Phys* 1989; 16:66-74
9. Humm JL, Cobb LM. Non-uniformity of tumour dose in radioimmunotherapy. *J Nucl Med* 1990; 31:75-83
10. Humm JL, Roeske JC, Fisher DR, Chen GT. Microdosimetric concepts in radioimmunotherapy. *Med Phys* 1993; 20:535-541
11. Leichner PK, Kwok CS. Tumour dosimetry in radioimmunotherapy: methods of calculation for beta particles. *Med Phys* 1993; 20:529-534
12. Howell RW. The MIRDSchema: From Organ to Cellular Dimensions. *J Nucl Med* 1994; 35:531-533
13. O'Donoghue JA. Implications of non-uniform tumour doses for radioimmunotherapy. *J Nucl Med* 1999; 40:1337-1341
14. Thierens HM, Monsieurs MA, Brans B, Van Driessche T, Christiaens I, Dierckx RA. Dosimetry from organ to cellular dimensions. *Comput Med Imaging Graph* 2001; 25:187-193

15. Bolch WE, Bouchet LG, Robertson JS, et al. MIRD pamphlet No. 17: The dosimetry of non-uniform activity distributions-radionuclide S values at the voxel level. *J Nucl Med* 1999; 40:11S-36S
16. Faraggi M, Gardin I, Stievenart JL, Bok BD, Guludec DL. Comparison of cellular and conventional dosimetry in assessing self-dose and cross-dose delivered to the cell nucleus by electron emissions of Tc-99m, I-123, In-111, Ga-67 and Tl-201. *Eur J Nucl Med* 1998; 25:205-214
17. ICRP No 23: Report of the Task Group on Reference Man, Chairman Snyder WS. Oxford New York Toronto Sydney Paris Frankfurt: Pergamon Press 1984
18. Sgouros G, Barest G, Thekkumthala J, et al. Treatment planning for internal radionuclide therapy three-dimensional dosimetry for non-uniformly distributed radionuclides. *J Nucl Med* 1990; 31:1884-1891
19. Valadon P. RasTop: Molecular Graphics Visualization Tools. 2002
20. Berger MJ. NISTIR 4999, National Institute of Standards and Technology, Gaithersburg, 1993
21. Johnson TK. MABDOS: a generalized program for internal dosimetry. *Comput Methods Programs Biomed* 1988; 37:159-167
22. Stabin MG. MIRDOSE: personal computer software for internal dose assessment in nuclear medicine. *J Nucl Med* 1996; 37:538-546
23. Coulot J, Ricard M, Aubert B. Validation of the EGS user code DOSE3D for internal beta dose calculation at the cellular and tissue levels. *Phys Med Biol* 2003; 48:2591-2602
24. Clairand I, Ricard M, Gouriou J, Di Paola M, Aubert B. DOSE3D: EGS4 Monte Carlo code-based software for internal radionuclide dosimetry. *J Nucl Med* 1999; 40:1517-1523
25. Furhang EE, Chui CS, Kolbert KS, Larson SM, Sgouros G. Implementation of a Monte Carlo dosimetry method for patient-specific internal emitter therapy. *Med Phys* 1997; 24:1163-1172
26. Kawrakow I, Fippel M, Friedrich K. 3D electron calculation using a Voxel based Monte Carlo algorithm (VMC). *Med Phys* 1996; 23:445-457
27. Liu A, Williams LE, Wong JY, Raubitschek AA. Monte Carlo-assisted voxel source kernel method (MAVSK) for internal beta dosimetry. *Nucl Med Biol* 1998; 25:423-433
28. Ilic RD. Computational simulation of electron penetration through material by Monte Carlo techniques. In: Milan Kurepa, eds. 100 Years since Discovery of Electron, Vol. VI. Belgrade: Serbian Academy of Sciences and Art (SANU); 1997:289-322
29. Altiparmakov DV, Belichev P. An efficiency study of the R - function method applied as solid modeler for Monte Carlo calculations. *Progres in Nuclear Energy* 1990; 24:77-88
30. Berger MJ. Monte Carlo calculation of the penetration and diffusion of fast charged particles. In: Berni Alder, eds. *Methods in computational physics Vol. I*. New York: Academic Press; 1963:135-215
31. Akkerman AF. Modelling of the charge particles trajectories in materials. Moscow: Energoatomizdat, 1991. (In Russian)
32. Landau L. On the energy loss of fast particles by ionisation. *J Phys (USSR)* 1940; 8:201-207
33. Blunck O, Leisegabg K. Zum Energieverlust schneller Elektronen in dinnen Schichten, *Z Phys* 1950; 128:500-505
34. Moliere G. Theorie der Streuung schneller geladener Teilchen II: Mehrfach - und Vielfachstreuung. *Z Naturforsch* 1948; 3a:78-97
35. Goudsmit S, Saunderson JL. Multiple scattering of electrons, *Phys. Rev* 1940; 57:21-29.
36. Bhabha HJ. The scattering of positrons by electrons with exchange on Dirac's theory of the positron. *Proc. Roy. Soc. (London)* 1936; A154:195
37. Negin CA, Worku G. RadDecay - Radioactive Nuclide Library and Decay Software, Version 4. Oak Ridge National Laboratory, Oak Ridge, Tennessee, 1993.
38. O'Donoghue JA, Bardies M, Whelton TE. Relations between Tumour Size and Curability for Uniformly Targeted Therapy with Beta-Emitting Radionuclides. *J Nucl Med* 1995; 36:1902-1909
39. Siegel JA, Stabin MG. Absorbed Fractions for Electrons and Beta Particles in Spheres of Various Sizes. *J Nucl Med* 1994; 35:152-156
40. Sgouros G, Chiu S, Pentlow KS, et al. Three-dimensional dosimetry for radioimmunotherapy treatment planning. *J Nucl Med* 1993; 34:1595-1601
41. Tagesson M, Ljungberg M, Strand SE. A Monte Carlo program converting activity distributions to absorbed dose distributions in a radionuclide treatment planning system. *Acta Oncol* 1996; 35:367-372
42. Siegel JA, Thomas SR, Stubbs JB, et al. MIRD Pamphlet No. 16. Techniques for quantitative radiopharmaceutical bio-distribution data acquisition and analysis for use in human radiation dose estimates. *J Nucl Med* 1999; 40:37S-61S
43. Makrigiorgos GM, Ito S, Baranowska-Kortylewicz J, et al. Inhomogeneous deposition of radiopharmaceuticals at the cellular level: experimental evidence and dosimetric implications. *J Nucl Med*. 1990; 31:1358-1363
44. Wheldon TE, O'Donoghue JA, Barrett A, Michalowski AS. The curability of tumours of differing size by targeted radiotherapy using I-131 or Y-90. *Radiotherapy and Oncology* 1991; 21:91-99
45. Hui TE, Fisher DR, Press OW, et al. Localized beta dosimetry of I-131 labelled antibodies in follicular lymphoma. *Med Phys* 1992; 19:97-104
46. Wessels BW, Siegel JA. Dosimetry Overview. *Cancer* 1997; 80:2501-2504